Apparent magnetic energy-barrier distribution in horse-spleen ferritin: Evidence for multiple interacting magnetic entities per ferrihydrite nanoparticle

T. G. St. Pierre,* N. T. Gorham, and P. D. Allen[†]

Department of Physics, The University of Western Australia, Crawley, WA 6009, Australia

J. L. Costa-Krämer[‡] and K. V. Rao

Department of Condensed Matter Physics, Royal Institute of Technology, S-100 44, Stockholm, Sweden

Magnetic viscosity measurements were made on native horse-spleen ferritin in zero applied magnetic field at temperatures between 2 and 21 K. The data have been used to calculate the apparent magnetic-moment-weighted energy barrier distribution for the sample of ferritin. The distribution is composed of a log-normal distribution plus a second distribution that is well described by an exponential decay of barrier frequency with increasing barrier height. The two distributions contribute approximately equally to the overall distribution. The log-normal distribution has its peak at an energy barrier of approximately 3×10^{-21} J, while the decay constant for the second distribution has a value of approximately 2×10^{-21} J. The existence of the low-energy barrier distribution with exponentially decaying shape in conjunction with the observation of shifted field-cooled magnetic hysteresis loops is interpreted as strong evidence for the existence of multiple interacting magnetic entities within each ferritin particle.

I. INTRODUCTION

Over the past decade the iron storage protein ferritin has featured prominently in a debate on whether or not resonant quantum tunneling of magnetization can be observed in bulk measurements on polydisperse mesoscopic antiferromagnetic particles.[1–13] Ferritin proteins each consist of a hollow approximately spherical shell of polypeptide with external diameter 12 nm and internal diameter 8 nm. Ferritin proteins isolated from biological systems are usually found to contain up to 4500 iron atoms within the central cavity in the form of a hydrated iron(III) oxyhydroxide particle (up to 8 nm in size) with trace amounts of phosphate. Horse-spleen ferritin has been the ferritin of choice for study since it is commercially available. Horse-spleen ferritin typically contains an average of 3000 Fe atoms per protein shell when highly loaded with iron.

Initial experiments designed to observe resonant quantum tunneling of the magnetization of horse-spleen ferritin particles were made at temperatures of approximately 30 mK by measuring the frequency-dependent magnetic noise and magnetic susceptibility of the particles using an integrated dc superconducting quantum interference device (SQUID) microsusceptometer.[1,2] A sharply defined resonance near 1 MHz was observed at temperatures up to 0.2 K. The data were interpreted in terms of macroscopic quantum tunneling of the weak magnetic moment of ferritin that is assumed to be coupled to the Néel vector of the generally antiferromagnetic iron(III) oxyhydroxide particles. The adjective "macroscopic" refers to the fact that the system being described is significantly larger than atomic-scale systems which are well described by quantum mechanics. The tunneling refers to the tunneling of the Néel vector through the magnetic anisotropy energy barrier that separates easy directions of magnetization for each particle. Although there were some objections to the interpretation of the microsusceptometer measurements in

terms of superpositions of macroscopic quantum states,[4,14,15] these discoveries prompted other researchers to look for additional phenomena that may be related to quantum tunneling of the ferritin moments.[3,7,8,12,13] Four basic phenomena have been identified for ferritin at temperatures above 1 K and have been interpreted in terms of quantum tunneling of magnetization in very small or zero applied fields. These phenomena are (a) temperature-independent magnetic viscosity S below a critical temperature (approximately 2 K),[3] (b) a nonmonotonic dependence of the superparamagnetic blocking temperature T_B on applied magnetic field H (temperatures of approximately 15 K),[7,8,12,13] (c) a maximum in the rate of change of magnetization M with H at zero applied field during constant rate sweeps of H (at temperatures between 5 and 13 K),[7,12] and (d) a nonmonotonic dependence of S on H at temperatures between 4 and 6.5 K with S increasing as H approaches zero.[7,12,13] Quantum tunneling is expected to be suppressed above a certain temperature owing to the interaction of the environment with the system.[16] Thus observations of these phenomena have important implications for the upper temperature limit at which quantum tunneling of magnetization can be observed. However, it has been pointed out by several workers that phenomena (a), (b), and (c) can also be explained in terms of classical models of magnetic particles.[9,11] Here we report data on the magnetic viscosity of ferritin that sheds further light on its magnetic relaxation processes at temperatures above 1 K.

II. MATERIALS AND METHODS

Native horse-spleen ferritin was obtained from Sigma Chemical Company in the form of an aqueous solution (50 mg ferritin/mL). An aliquot of the ferritin was diluted to 1 mg/mL, and a drop of this diluted solution was allowed to air dry on a carbon film supported by a 400-mesh copper transmission electron microscope (TEM) grid. TEM images of the

mineral cores of the ferritin protein molecules were obtained using a Jeol 2000 FX TEM operating at 80 keV. The core size distribution was measured by photographically enlarging the TEM images and measuring the largest and smallest dimension of each core ($n = 100$) in the enlarged image using vernier callipers. Selected-area electron diffraction patterns were recorded from several regions on the TEM grid yielding powder diffraction patterns.

A sample of the concentrated ferritin solution was freeze dried. The iron content of the freeze-dried powder was determined using atomic absorption spectrometry and was found to be $10.7 \pm 0.5\%$ by mass. A sample of the dried protein was then gently compressed into a cylindrical pellet (diameter 4 mm, length approximately 1 mm, mass 0.0216 g). Magnetic measurements were made on the pellet using a SQUID-based magnetometry system with superconducting solenoid (Quantum Design MPMS-7). Magnetic viscosity measurements were made in near zero field (approximately 2 Oe) over a range of temperatures from 2.0 K up to 21.0 K. Temperature measurements were made using a germanium resistance thermometer.

For each measurement of the magnetic viscosity parameter S, the sample was thermally demagnetized at 50 K or above and then cooled in zero field to the target temperature. A large (70 kOe) field was then applied and subsequently removed (by ramping down the current in the coils of the solenoid and then briefly heating the coils above their critical temperature to quench any remaining current) to yield a remanent magnetic moment on the sample. The evolution of the remanent magnetic moment was then monitored over a period of approximately 10^3 s. All measurements of S at or below temperatures of 10 K were made at least twice in order to reduce the possibility of random instrumental error affecting the measurements.

Both zero-field-cooled and field-cooled magnetic hysteresis loops were measured at 5 K by cooling the sample in zero field and then sweeping the applied field to 70 kOe and back to -70 kOe and by cooling the sample from 300 K in 70 kOe before sweeping the field.

An ^{57}Fe Mössbauer spectrum of the sample at 5 K was also recorded.

III. EXPERIMENTAL RESULTS

TEM images of the native horse-spleen ferritin showed well-dispersed electron dense particles qualitatively similar to those reported elsewhere.[17,18] The mean aspect ratio of the particle images was 1.2, suggesting that the mineral cores of the ferritin molecules were approximately spherical. The mean effective diameter of the cores was 6.39 nm with a standard deviation of 0.78 nm. Powder electron diffraction patterns from the ferritin cores yielded lattice spacings of 0.255, 0.224, 0.173, 0.147, 0.106, 0.092, 0.088, and 0.085 nm consistent with those reported previously for the ferrihydrite mineral cores of horse-spleen ferritin.[19]

Figure 1 shows the decay with time of the remanent specific magnetization of the freeze-dried ferritin sample after removal of a 70-kOe applied magnetic field at a series of different temperatures ranging from 2.0 K up to 21.0 K. The
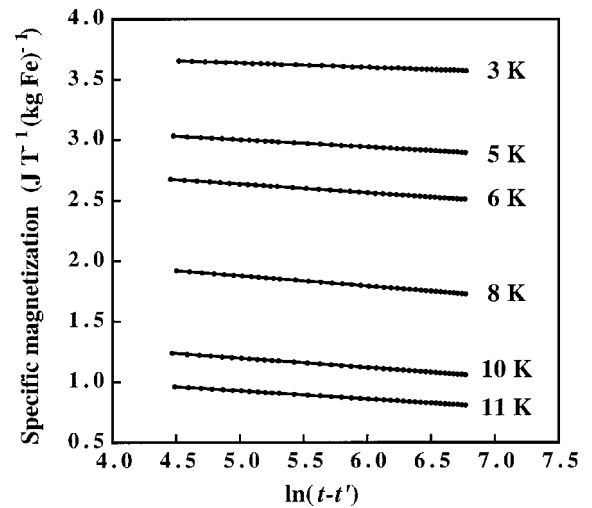

FIG. 1. Specific magnetization of the iron in native horse-spleen ferritin against $\ln(t - t')$ at temperatures near the maximum in $S(T)$. The solid circles are experimentally measured data points on the ferritin in zero field after removal of a 70-kOe applied field. The solid lines are fits of Eq. (1) to the data. t' is obtained from fits of Eq. (1) to the experimental data.

data appear to be well described by a linear decay of magnetic moment with the logarithm of time. The solid lines in Fig. 1 are least-squares fits of the equation

$$\sigma(t) = \sigma_0 - S \ln(t - t') \tag{1}$$

to the data, where $\sigma(t)$ is the specific magnetization of the sample at universal time t and σ_0, S, and t' are variable parameters in the fitting procedure. The magnetic viscosity parameter S is plotted against temperature in Fig. 2. At high temperatures (>25 K), S is zero. As the temperature is lowered, S increases to a maximum at approximately 8 K and then starts to decrease again. By 2 K, S appears to be tending towards a nonzero value as absolute zero of temperature is approached.
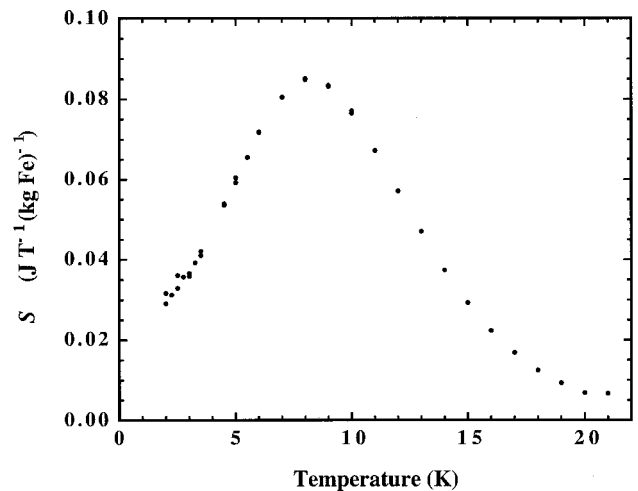

FIG. 2. Magnetic viscosity parameter S plotted against temperature for a sample of native horse-spleen ferritin.

The results of zero-field-cooled and field-cooled magnetic hysteresis measurements at 5 K are almost identical to those measured by Makhlouf *et al.*[20] The zero-field-cooled magnetic field sweep results in a coercive field of approximately 2.5 kOe, while the field-cooled sweep results in a shift of the loop by approximately 0.3 kOe.

The Mössbauer spectrum of the horse-spleen ferritin sample at 5 K consisted of a superposition of a sextet and a doublet with parameters very similar to those measured by other workers.[21] The sample measured in the present study yielded a spectrum with the doublet contributing 7% to the total spectral area.

IV. MAGNETIC VISCOSITY AND ENERGY-BARRIER DISTRIBUTIONS

Magnetic viscosity is the change in magnetization with time of a system held in a constant applied magnetic field H.[22] This time dependence of magnetization either is due to the thermal activation of the magnetization direction of metastable magnetic entities over energy barriers (leading to temperature dependent magnetic viscosity) or due to quantum-mechanical tunneling of the magnetization through the energy barriers (leading to temperature-independent magnetic viscosity and nonzero viscosity near absolute zero of temperature).

First, we will describe the relationship between the magnetic viscosity of a system in zero applied field and the magnetic activation energy-barrier distribution within the system assuming that all relaxation processes are thermally activated. Later, we will discuss the effect that quantum tunneling of the magnetization vector of each magnetic entity may have on the experimentally observed magnetic viscosity.

Generally, for a system with a broad and slowly varying distribution of energy barriers ΔE, the time dependence of magnetization M or specific magnetization σ of the system is well described by the relation[22]

$$\sigma(H,t) = \sigma_0(H) - S(H)\ln(t - t'), \qquad (2)$$

where $S(H)$, $\sigma_0(H)$, and t' are experimentally derived parameters. Note that Eq. (1) is related to the zero field ($H = 0$) case of Eq. (2). Thus it appears that the magnetization processes giving rise to the magnetic viscosity observed in ferritin are due to a broad distribution of activation energy barriers in the system. The magnetic viscosity behavior of a system of an ensemble of magnetic entities, each with a characteristic magnetic moment and activation energy barrier can be discussed in the following terms.

For an ensemble of magnetic entities in metastable states with identical activation energy barriers ΔE, there is a characteristic relaxation time τ at temperature T owing to thermal activation over the energy barriers. The relaxation time τ is related to temperature by the Néel-Arrhenius law[23]

$$\tau = \tau_0 e^{\Delta E/kT}, \qquad (3)$$

where k is the Boltzmann constant and τ_0 is a characteristic time constant, which is of the order of $10^{-11} - 10^{-12}$ s for native horse-spleen ferritin.[24–26] An ensemble of such enti-

ties would then be expected to show an exponential decrease in magnetic moment with time after removal of an applied static field. As noted earlier, however, a system with a range of activation energy barriers can lead to a linear decay of its magnetic moment with the logarithm of time because of the resulting spread in relaxation times within the system.

Thus once the static field has been completely removed, there will be a critical energy-barrier size ΔE_c above which a magnetic entity essentially will be stable because of the rapid increase of τ with ΔE [Eq. (3)]. The size of ΔE_c increases with time in the following way:

$$\Delta E_c = \ln\left(\frac{t - t^*}{\tau_0}\right)kT, \qquad (4)$$

where t^* is a point in time somewhere between the start and finish of the ramping down of the applied field. For magnetic entities with $\Delta E < \Delta E_c$, τ will be much less than $(t - t^*)$ and rapid thermal activation of the magnetic moments of these entities will average their moments to zero, and hence they will not contribute to the magnetic moment of the system in zero applied field.

In order to calculate the remanent specific magnetization of the system at time t during the observation, the distribution of activation energy barriers within the system must be taken into account. The magnetic moment of the system changes as a function of time because ΔE_c is a function of time [Eq. (4)]. Thus, for a system that has recently had a saturating applied field removed, the specific magnetization of the system at the start of the observation time ($t = t_0$) can be written as

$$\sigma(t_0) = \int_{\Delta E_c(t_0)}^{\infty} q(\Delta E)d\Delta E, \qquad (5)$$

where $q(\Delta E)d\Delta E$ is the quantity of magnetic moment per unit mass of specific element (e.g., iron) in the system that resides on entities with activation energy barriers between ΔE and $\Delta E + d\Delta E$. The value of $\Delta E_c(t_0)$ in Eq. (5) is determined by the time delay between removal of the applied field and the commencement of observation of the magnetic moment of the system and by the rate of change of applied field during its removal. The latter factor influences the value of t^* in Eq. (4).

The evolution of the observed specific magnetization of the system as a function of time t can then be written as

$$\sigma(t) = \sigma(t_0) - \int_{\Delta E_c(t_0)}^{\Delta E_c(t)} q(\Delta E)d\Delta E. \qquad (6)$$

Equation (4) can be used to rewrite Eq. (6) as follows:

$$\sigma(t) \approx \sigma(t_0) - kT[\ln(t - t^*)$$
$$- \ln(t_0 - t^*]q\left(\frac{\Delta E_c(t) - \Delta E_c(t_0)}{2}\right) \qquad (7)$$

where $\Delta E_c(t^*) \equiv 0$.

For typical experimental time scales, $\Delta E_c(t) - \Delta E_c(t_0) \ll \Delta E_c(t)$. For example, a typical magnetometery measurement on ferritin would have $t - t_0 = \tau_{obs} \approx 1000$ s, with t_0

$-t^*$ being approximately 10 s, yielding a value of $[\Delta E_c(t) - \Delta E_c(t_0)]/\Delta E_c(t)$ of 0.14 (0.12 for $t_0 - t^* = 20$ s, 0.11 for $t_0 - t^* = 30$ s, taking τ_0 to be 5×10^{-12} s. Thus, if $q(\Delta E)$ is a slowly and smoothly varying function of ΔE,

$$q(\Delta E_c(t_0)) \approx q(\Delta E_c(t))$$

$$\approx q\left(\frac{\Delta E_c(t) + \Delta E_c(t_0)}{2}\right)$$

$$\approx q(\langle \Delta E_c \rangle),$$

where $q([\Delta E_c(t) + \Delta E_c(t_0)]/2)$ is an approximate average of the value of $q(\Delta E_c)$ over the range $q(\Delta E_c(t_0))$ to $q(\Delta E_c(t))$ and $\langle \Delta E_c \rangle$ is the mean critical energy barrier probed by the measurement.

So Eq. (7) can be rewritten as

$$\sigma(t) = [\sigma(t_0) + q(\langle \Delta E_c \rangle) kT \ln(t_0 - t^*)]$$

$$- [q(\langle \Delta E_c \rangle) kT] \ln(t - t^*). \quad (8)$$

Inspection of Eq. (8) shows that it has the same form as Eq. (1) with S being given by

$$S = -\frac{d\sigma}{d\ln(t - t^*)} = q(\langle \Delta E_c \rangle) kT. \quad (9)$$

Thus it is apparent from Eq. (9) that S/kT is a measure of $q(\langle \Delta E_c \rangle)$.

Recall that during measurements of S carried out with identical field ramping rates and times of observation, ΔE_c is proportional to kT [Eq. (4)] with the constant of proportionality being $C \equiv \ln(t - t^*/\tau_0)$.

In other words $(S/kT)d(CkT)$ is a measure of $q(\langle \Delta E_c \rangle)d(\Delta E_c)$ which is the quantity of magnetic moment per unit mass of specific element in the system which experiences energy barriers between CkT and $CkT + dCkT$. Thus, by measuring S/kT at different values of T, $q(\Delta E_c)$ is being measured at different values of ΔE_c.

So a plot of S/kT against CkT (Fig. 3) represents the activation energy barrier distribution of the system weighted by the quantity of magnetic moment per unit mass of specific element associated with each activation energy value. The value of C used to calculate the values along the abscissa was taken to be 32.5 ± 0.5 using the values of $\ln(\tau_0)$ for horse-spleen ferritin reported previously.[24,25,27]

It is worth noting that the same analysis of experimental data can be used even if the applied field that is removed is not saturating (as is the case for the measurements presented here). If the applied field is less than saturating, then the remanent magnetic moment of the system will be less. However, the missing amount of moment would not contribute to the measurement of S over the limited experimental time scale because it would be associated with larger energy barriers. Furthermore, measurements of S at higher temperatures (where the larger barriers are being sampled) would result in this missing moment being recovered because it will be reoriented by the applied field owing to thermal activation at these higher temperatures. Thus it is only necessary for the applied field to reverse the magnetic moment of entities with
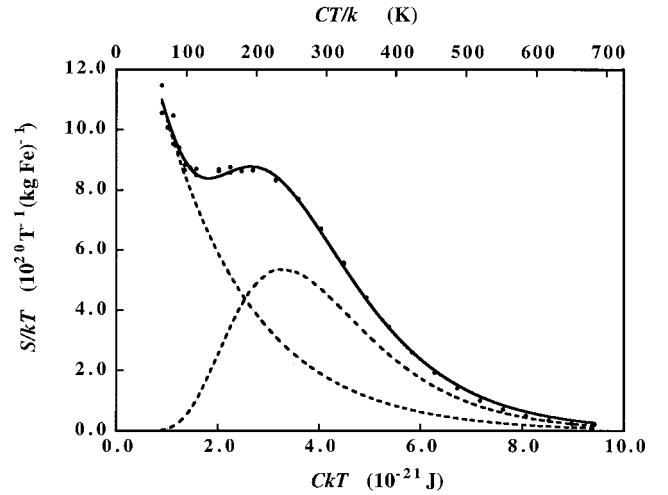

FIG. 3. Plot of S/kT against CkT for native horse-spleen ferritin represents the apparent specific-magnetization-weighted energy, barrier distribution for the sample. The solid circles are experimentally measured data points. The solid curve is a fit of Eq. (10) to the data with the dashed lines illustrating the log-normal and exponential decay components of the fit.

energy barriers between ΔE_c and $\Delta E_c + d\Delta E_c$ corresponding to the temperature and time of observation of the measurement [see Eq. (4)]. This requirement will always be fulfilled since application of an applied field will always reduce the energy barrier that the moment needs to overcome in order to gain greater alignment with the direction of the applied field. Thus, if the moment of the entity has a certain probability of flipping in zero field during the experimental observation, it will have a much greater probability of flipping towards an applied field no matter how small is the applied field.

Finally, it should be noted that several researchers have proposed that quantum tunneling of the macroscopic magnetic moment on each ferritin particle may be responsible for the observed magnetic relaxation behavior of ferritin at low temperatures.[28] In such models, the magnetic entities within the system are considered to be noninteracting. Theories of quantum tunneling of the magnetic moment predict a critical temperature known as the crossover temperature T_c. Above T_c the magnetic entity is considered to relax by thermal activation processes as described above, whereas below T_c the magnetic moment of the entity may quantum mechanically tunnel from one orientation to another. The manifestation of such quantum tunneling phenomena modifies the above description of the relationship between magnetic viscosity and activation energy barrier distributions by replacing the absolute temperature T in Eq. (4) with an effective temperature T^* where $T^* = T$ at temperatures above T_c and $T^* = T_c$ at temperatures below T_c. The end result is that the magnetic viscosity is predicted to be independent of temperature below T_c.[28] Thus, if quantum tunneling of the magnetization vector was manifested in ferritin, S/kT would be expected to vary as $1/T$ below the crossover temperature and may not necessarily reflect the energy barrier distribution within the system.

V. DISCUSSION

The transmission electron microscopy data and electron diffraction data are very similar to those measured by other workers for horse-spleen ferritin,[17–19] confirming the presence of well-separated ferrihydrite nanoparticles in the sample. However, our measurement of the iron content is perhaps somewhat smaller than is usually found in horse-spleen ferritin. This is supported by the fact that the Mössbauer spectrum of our sample at 5 K yielded a doublet accounting for 7% of the total spectral area. Previous Mössbauer spectroscopic measurements on horse-spleen ferritin at 4.2 K (Refs. 21 and 24) have shown the doublet to be extinguished, thus implying that the sample of horse-spleen ferritin in the present study contains particles that may be smaller than usual for horse-spleen ferritin. It should be noted that even within one animal species, the size and degree of structural order within the ferrihydrite nanoparticles of ferritin can vary considerably depending on factors such as the state of health of the animal and from which organ the ferritin was isolated.[29] The density of the ferrihydrite particles also is known to vary depending on factors such as the degree of hydration, phosphate content, and degree of structural order within the particles.[30]

The magnetic viscosity behavior observed here in zero field is also qualitatively similar to that previously observed for horse-spleen ferritin in applied fields.[3] We observe a peak in S near 8 K and we also observe a change in sign of the second derivative of S with T at around 4.5 K. However, the plot of S/kT against CkT (Fig. 3) represents the apparent activation energy barrier distribution within the sample of ferritin weighted by the amount of magnetic moment experiencing each energy barrier height. This is the first time that the apparent energy-barrier distribution for ferritin has been measured. The data clearly show that there is more than one contribution to the energy-barrier distribution. For a simple picture of an ensemble of thermally activated single-domain superparamagnetic particles with each particle undergoing coherent reversal of magnetization during activation, one would expect a log-normal distribution of energy barriers. The log-normal distribution takes into account such factors as the distribution of particle sizes and distribution of magnetic moments in the ensemble. However, in order to fit adequately a log-normal distribution to the data, another component to the distribution clearly is required (Fig. 3). We have found that an exponentially decaying curve, when added to the log-normal distribution, provides an adequate fit to the data (although a second log-normal distribution also gives a reasonable fit). Interestingly, it was not possible to obtain a good fit with a curve decaying as $1/T$. The solid line in Fig. 3 is a fit of the equation

$$q(\Delta E) = q_1(\Delta E) + q_2(\Delta E)$$

$$= q_1 \exp\left\{\frac{-[\ln(\Delta E) - \ln(\Delta E_1)]^2}{2[\Delta \ln(\Delta E)]^2}\right\} + q_2 \exp\left\{\frac{-\Delta E}{\Delta E_2}\right\}$$

(10)

to the data, where $q_1(\Delta E)$ is the log-normal distribution and $q_2(\Delta E)$ is the exponentially decaying distribution of energy barriers ΔE, q_1 is the maximum value of $q_1(\Delta E)$, ΔE_1 is the most frequently occurring energy barrier in the log-normal distribution, $\Delta \ln(\Delta E)$ is the width of the log-normal distribution, q_2 is the value of the exponential distribution extrapolated to the zero-energy barrier, and ΔE_2 is the decay constant of the exponential distribution that characterizes how rapidly the distribution decreases with increasing energy barrier height. The fit yields the following parameters: $q_1 = (5.4 \pm 0.5) \times 10^{20} \, \text{T}^{-1} \, (\text{kg Fe})^{-1}$, $\Delta E_1 = (3.28 \pm 0.04) \times 10^{-21} \, \text{J}$ or $\Delta E_1/k = 238 \pm 3 \, \text{K}$; $\Delta \ln(\Delta E) = 2.48 \pm 0.12$, $q_2 = (1.81 \pm 0.13) \times 10^{21} \, \text{T}^{-1} \, (\text{kg Fe})^{-1}$, and $\Delta E_2 = (1.8 \pm 0.2) \times 10^{-21} \, \text{J}$ or $\Delta E_2/k = 130 \pm 17 \, \text{K}$. The uncertainties on each of these parameters are those returned by the Levenberg-Marquardt algorithm used to fit the curve. This algorithm uses the assumption that the fitted parameters are described by multivariate normal distribution. Thus the true experimental uncertainties are likely to be somewhat larger and will include a systematic error of at least 2% on values of ΔE owing to the uncertainty on the value of C. The energy-barrier distribution that we measure spans the estimates of the mean energy barrier for horse-spleen ferritin measured by other workers [$\Delta E/k = 318 \, \text{K}$ (Ref. 25) and $\Delta E/k = 400 \, \text{K}$ (Ref. 26)] and that inferred by Dickson *et al.*[24] ($\Delta E/k = 288 \, \text{K}$) and Mohie-Eldin *et al.*[31] ($\Delta E/k = 244 \, \text{K}$). It is worth noting that the iron content of the horse-spleen ferritin studied by Allen *et al.* was 23% by mass compared with the 10.7% by mass in the sample in the present study. Both samples were obtained from the same supplier, but were different batches. This may explain why Allen *et al.*[26] measured a relatively high value for $\Delta E/k$.

In order to make a self-consistency check, we have numerically integrated the area under the experimentally measured specific-magnetization-weighted energy barrier distribution (Fig. 3) from $8.97 \times 10^{-22} \, \text{J}$ upwards. The value of $8.97 \times 10^{-22} \, \text{J}$ corresponds to the lowest-energy barrier measured: i.e., the results of the measurements at 2 K. Thus the integral of the curve from $8.97 \times 10^{-22} \, \text{J}$ upwards should yield the initial remanent specific magnetization measured at 2 K because it represents the blocked specific magnetization at 2 K. The integral under the curve was found to be 3.87 $\text{J T}^{-1} \, (\text{kg Fe})^{-1}$, while the initial measurement of specific magnetization of the ferritin at 2 K immediately after removing the 70-kOe field was 3.95 $\text{J T}^{-2} \, (\text{kg Fe})^{-1}$ giving an agreement within 2% [NB: $1 \, \text{J T}^{-1} \, (\text{kg Fe})^{-1} = 1 \, \text{emu} \, (\text{g Fe})^{-1}$].

The origin of the log-normal component of the energy-barrier distribution most likely is due to the distribution of particle volumes and moments within the ensemble. There is not a unique relationship between particle volume and moment per particle for ferritin, but on average the moment rises with the square root of the number of Fe atoms within the core.[32] The origin of the second component of the energy-barrier distribution is less clear. However, it is interesting to note that atomic-scale magnetic modeling of ferrimagnetic nanoparticles with surface roughness[33] resulted in energy-barrier distributions qualitatively similar to the exponentially decaying distribution that we have measured for horse-spleen ferritin. Thus it is possible that the exponentially decaying contribution to the energy-barrier distribution

is due to surface spins or small groups of surface spins that are less strongly coupled to the internal core of the ferritin mineral particles. Previous studies of energy-barrier distributions in nanoparticles of $BaFe_{10.4}Co_{0.8}Ti_{0.8}O_{19}$ M-type doped barium ferrite[34] found a minor low barrier component to the energy-barrier distribution in addition to a major log-normal component. The low barrier contribution was modeled as a second log-normal distribution around lower-energy barriers and was attributed to the presence of weak demagnetizing interactions between the particles. In our study of horse-spleen ferritin, the low-energy barrier component of the distribution has a contribution to the overall distribution that is approximately equal to that of the higher-energy barrier log-normal component. The relatively large contribution of the low-energy barrier distribution may be due to the fact that the majority of the excess spin of ferritin particles is expected to be at the surface where the density of uncompensated spins is likely to be higher. Thus the magnetic entities (individual spins or clusters of coupled spins) at the surface of ferritin mineral particles are likely to contribute far more per Fe atom to the magnetic-moment-weighted energy-barrier distribution than the magnetic entities within the cores of the particles which are likely to have a much lower magnetic moment per Fe atom (owing to a more complete compensation of spins within each entity). This picture of the magnetic structure of horse-spleen ferritin is consistent with the model proposed by Brooks *et al.*[35] based on variable-temperature magnetic susceptometry measurements.

The value of $\Delta E_c/k$ for ^{57}Fe Mössbauer spectroscopy at 5 K is 32 K, which is an energy barrier lower than any we have measured by magnetic viscosity observations. The presence of the doublet in the spectrum indicates that approximately 7% of the Fe atoms in the sample are within magnetic entities that experience energy barriers less than 32 K. Thus the magnitude of the Mössbauer spectral doublet at 5 K is consistent with the magnetometery measurements.

Another possible interpretation of the low-energy barrier contribution to the apparent energy-barrier distribution could be that quantum tunneling of the magnetic moments of the ferritin particles is being manifested. As mentioned earlier, theories of the macroscopic quantum tunneling of the magnetization vector of small particles predict that S/kT should decrease as $1/T$ as the temperature is increased up until the crossover temperature T_c. This behavior is qualitatively observed in our data, although we were not able to obtain a good fit of a sum of a log-normal curve and a $1/T$ curve to the data. It may be possible to explain the data in terms of a distribution of T_c values.

A further possible interpretation of the existence of two distinct distributions of magnetic anisotropy energy barriers is in terms of different species of ferritin mineral particles. Recent electron nanodiffraction measurements on individual horse-spleen ferritin mineral particles[36] has shown that while the majority have a hexagonal structure generally considered to be the major phase in ferrihydrite, several minor phases are present including some that are similar in structure to the iron oxides magnetite and hematite and also some composed of a highly disordered material. In general, each core was observed to consist of one single crystal of one phase. If the cores that have a structure similar to the mineral magnetite also have a magnetization similar to magnetite, then they will contribute disproportionally to the magnetic-moment-weighted energy-barrier distribution. Thus it could be that one distribution belongs to the ferrihydrite particles while the other belongs to magnetite-like particles. This theory could be tested by making zero-field magnetic viscosity measurements on ferritin before and after passage through a magnetic separation column.

On balance, we prefer an interpretation of the data in terms of multiple magnetic entities per ferritin particle. This interpretation fits better with the observations by us and others[20] of shifted magnetic hysteresis loops after cooling horse-spleen ferritin in an applied magnetic field. These shifted loops are an indication of the presence of exchange anisotropy within the system under observation. Since the nanoparticles are well separated by the protein shells, the exchange anisotropy must arise from interactions between independent magnetic entities within each ferritin nanoparticle. It seems likely that the exchange anisotropy arises from exchange interactions between the clusters of surface spins (with small energy barriers) and the low-moment cores (with generally larger energy barriers).

In conclusion, we have measured the apparent specific-magnetization-weighted energy-barrier distribution in horse-spleen ferritin and have found that it is composed from two distinct distributions. The evidence strongly points towards the existence of multiple interacting magnetic entities within each ferritin mineral nanoparticle. These entities should be taken into account in any models developed to describe the dynamic magnetic behavior of ferritin, whether the models be based on quantum tunneling or on classical thermal activation of magnetization.

---

*Corresponding author. +61-8-9380-2747 FAX: +61-8-9380-1014. Electronic address: stpierre@physics.uwa.edu.au

†Present address: Department of Brain and Cognitive Sciences, 168 Meliora Hall, University of Rochester, Rochester, NY 14627.

‡Present address: Instituto de Microelectrónica de Madrid, CSIC-CNM (Consejo Superior de Investigaciones Científicas-Centro Nacional de Microelectrónica), Isaac Newton, 8-Parque Tecnológico de Madrid, 28760 Tres Cantos, Madrid, España.

[1] D. D. Awschalom, J. F. Smyth, G. Grinstein, D. P. DiVincenzo, and D. Loss, Phys. Rev. Lett. **68**, 3092 (1992).

[2] D. D. Awschalom, D. P. DiVincenzo, and J. F. Smyth, Science **258**, 414 (1992).

[3] J. Tejada and X. X. Zhang, J. Phys.: Condens. Matter **6**, 263 (1994).

[4] A. Garg, Phys. Rev. Lett. **74**, 1458 (1995).

[5] S. Gider, D. D. Awschalom, T. Douglas, K. Wong, S. Mann, and G. Cain, J. Appl. Phys. **79**, 5324 (1996).

[6] S. Gider, D. D. Awschalom, T. Douglas, S. Mann, and M. Chaparala, Science **268**, 77 (1995).

[7] J. Tejada, X. X. Zhang, E. del Barco, J. M. Hernandez, and E. M. Chudnovsky, Phys. Rev. Lett. **79**, 1754 (1997).

[8] J. R. Friedman, U. Voskoboynik, and M. P. Sarachik, Phys. Rev. B **56**, 10 793 (1997).

[9] R. Sappey, E. Vincent, N. Hadacek, F. Chaput, J. P. Boilot, and D.

Zins, Phys. Rev. B **56**, 14 551 (1997).

[10] E. M. Chudnovsky, J. Magn. Magn. Mater. **185**, L267 (1998).

[11] M. Hanson, C. Johansson, and S. Mørup, Phys. Rev. Lett. **81**, 735 (1998).

[12] E. del Barco, F. Luis, J. Tejada, X. X. Zhang, J. Bartolome, J. M. Hernandez, and E. M. Chudnovsky, J. Appl. Phys. **83**, 6934 (1998).

[13] F. Luis, E. del Barco, J. M. Hernandez, E. Remiro, J. Bartolome, and J. Tejada, Phys. Rev. B **59**, 11 837 (1999).

[14] A. Garg, Phys. Rev. Lett. **71**, 4249 (1993).

[15] A. Garg, J. Appl. Phys. **76**, 6168 (1994).

[16] N. V. Prokof'ev and P. C. E. Stamp, Rep. Prog. Phys. **63**, 669 (2000).

[17] W. H. Massover, Micron **24**, 389 (1993).

[18] S. Mann, J. M. Williams, A. Treffry, and P. M. Harrison, J. Mol. Biol. **198**, 405 (1987).

[19] P. M. Harrison, F. A. Fischbach, T. G. Hoy, and G. H. Haggis, Nature (London) **216**, 1188 (1967).

[20] S. A. Makhlouf, F. T. Parker, and A. E. Berkowitz, Phys. Rev. B **55**, 14 717 (1997).

[21] J. F. Boas and B. Window, Aust. J. Phys. **19**, 573 (1966).

[22] R. Street and J. C. Woolley, Proc. Phys. Soc., London, Sect. A **52**, 562 (1949).

[23] L. Néel, Ann. Geophys. (C.N.R.S.) **5**, 99 (1949).

[24] D. P. E. Dickson, N. M. K. Reid, C. Hunt, H. D. Williams, M. Elhilo, and K. O'Grady, J. Magn. Magn. Mater. **125**, 345 (1993).

[25] S. H. Kilcoyne and R. Cywinski, J. Magn. Magn. Mater. **140-144**, 1466 (1995).

[26] P. D. Allen, T. G. St. Pierre, W. Chua-anusorn, V. Ström, and K. V. Rao, Biochim. Biophys. Acta **1500**, 186 (2000).

[27] P. D. Allen, T. G. St. Pierre, and R. Street, J. Magn. Magn. Mater. **177-181**, 1459 (1998).

[28] E. M. Chudnovsky and J. Tejada, *Macroscopic Quantum Tunneling of the Magnetic Moment* (Cambridge University Press, Cambridge, England, 1998).

[29] T. G. St. Pierre, K. C. Tran, J. Webb, D. J. Macey, B. R. Heywood, N. H. Sparks, V. J. Wade, S. Mann, and P. Pootrakul, Biol. Met. **4**, 162 (1991).

[30] T. G. St. Pierre, J. Webb, and S. Mann, in *Biomineralization: Chemical and Biochemical Perspectives*, edited by S. Mann, J. Webb, and R. J. P. Williams (VCH, Weinheim, 1989), pp. 295–344.

[31] M.-E. Y. Mohie-Eldin, R. B. Frankel, and L. Gunther, J. Magn. Magn. Mater. **135**, 65 (1994).

[32] J. G. E. Harris, J. E. Grimaldi, D. D. Awschalom, A. Chiolero, and D. Loss, Phys. Rev. B **60**, 3453 (1999).

[33] R. H. Kodama and A. E. Berkowitz, Phys. Rev. B **59**, 6321 (1999).

[34] X. Batlle, M. G. del Muro, and A. Labarta, Phys. Rev. B **55**, 6440 (1997).

[35] R. A. Brooks, J. Vymazal, R. B. Goldfarb, J. W. M. Bulte, and P. Aisen, Magn. Reson. Med. **40**, 227 (1998).

[36] J. M. Cowley, D. E. Janney, R. C. Gerkin, and P. R. Buseck, J. Struct. Biol. **131**, 210 (2000).